

Apatinib Combined with Local Irradiation Leads to Systemic Tumor Control via Reversal of Immunosuppressive Tumor Microenvironment in Lung Cancer

Li-jun Liang, MD¹
Chen-xi Hu, MS¹
Yi-xuan Wen, MM¹
Xiao-wei Geng, MM²
Ting Chen, MM¹
Guo-qing Gu, MD¹
Lei Wang, MD¹
You-you Xia, MD¹
Yong Liu, MS¹
Jia-yan Fei, MM¹
Jie Dong, MM³
Feng-hua Zhao, MM¹
Yiliyar Ahongjiang, MM⁴
Kai-yuan Hui, PhD¹
Xiao-dong Jiang, MD¹

¹Department of Oncology, The Affiliated Lianyungang Hospital of Xuzhou Medical University, Lianyungang, ²Department of Clinical Medicine, Xuzhou Medical University, Xuzhou, ³Department of Clinical Pharmacology, The Affiliated Lianyungang Hospital of Xuzhou Medical University, Lianyungang, ⁴Medical Imaging Faculty of Xuzhou Medical University, Xuzhou, China

Correspondence: Xiao-dong Jiang, MD
Department of Oncology, The Affiliated Lianyungang Hospital of Xuzhou Medical University, Lianyungang 222000, China
Tel: 86-0518-85605722
Fax: 86-0518-85456700
E-mail: jxdpaper@163.com

Co-correspondence: Kai-yuan Hui, PhD
Department of Oncology, The Affiliated Lianyungang Hospital of Xuzhou Medical University, Lianyungang, 222000, China
Tel: 86-18961327098
Fax: 86-0518-85456700
E-mail: kyhui1987@163.com

Received May 28, 2019
Accepted September 2, 2019
Published Online September 2, 2019

*Li-jun Liang, Chen-xi Hu, and Yi-xuan Wen contributed equally to this work.

Purpose

This study aimed to investigate the potential systemic antitumor effects of stereotactic ablative radiotherapy (SABR) and apatinib (a novel vascular endothelial growth factor receptor 2 inhibitor) via reversing the immunosuppressive tumor microenvironment for lung carcinoma.

Materials and Methods

Lewis lung cancer cells were injected into C57BL/6 mice in the left hindlimb (primary tumor; irradiated) and in the right flank (secondary tumor; nonirradiated). When both tumors grew to the touchable size, mice were randomly divided into eight treatment groups. These groups received normal saline or three distinct doses of apatinib (50 mg/kg, 150 mg/kg, and 200 mg/kg) daily for 7 days, in combination with a single dose of 15 Gy radiotherapy or not to the primary tumor. The further tumor growth/regression of mice were followed and observed.

Results

For the single 15 Gy modality, tumor growth delay could only be observed at the primary tumor. When combining SABR and apatinib 200 mg/kg, significant retardation of both primary and secondary tumor growth could be observed, indicated an abscopal effect was induced. Mechanism analysis suggested that programmed death-ligand 1 expression increased with SABR was counteracted by additional apatinib therapy. Furthermore, when apatinib was combined with SABR, the composition of immune cells could be changed. More importantly, this two-pronged approach evoked tumor antigen-specific immune responses and the mice were resistant to another tumor rechallenge, finally, long-term survival was improved.

Conclusion

Our results suggested that the tumor microenvironment could be managed with apatinib, which was effective in eliciting an abscopal effect induced by SABR.

Key words

Apatinib, Stereotactic ablative radiotherapy, Anti-angiogenesis, PD-L1, Abscopal effect

Introduction

Ionizing radiation therapy is an effective approach to local tumor control. It plays an indispensable role in the treatment of non-small cell lung cancer (NSCLC) and other types of cancer. However, for metastatic lesions, radiotherapy is always limited to palliative symptoms and improvement of quality of life. Stereotactic ablative radiotherapy (SABR) optimizes local control by providing tumor-ablative doses with minimal damage to adjacent normal tissues and organs [1]. Accumulating evidence has shown that, SABR, delivered 1 to 3 fractions, can alter the inflammatory tumor microenvironment to trigger adaptive immune responses [2], which finally mediates tumor regression. One such observation is defined as “abscopal effect” and referred to nonirradiated tumor partial or complete eradication, suggesting an indirect systemic antitumor effect primed by local SABR [3]. This effect has been reported to date in NSCLC [4], melanoma [5], and other tumor species [6].

However, the incidence of abscopal effect is infrequent, and it has only been reported in a few cases. This may be because individual radiotherapy is generally unable to overcome the immunosuppressive factors of tumor-bearing host, including regulatory T cells (Tregs), myeloid-derived suppression cells (MDSC), and immuno-checkpoint (programmed death 1/programmed death-ligand 1 [PD-1/PD-L1] axis and cytotoxic T-lymphocyte antigen 4) [7]. Current strategies include radiotherapy combined with other regimens, such as Tregs depletion [8], cytokine addition [9], and in particular, combined with the PD-1/PD-L1 inhibitors. Given the recent success of cancer immunotherapy, SABR-induced abscopal effects may become widely seen [10,11].

Apatinib, a novel small molecule tyrosine kinase inhibitor (TKI), exerts its antitumor effects by specifically acting on vascular endothelial growth factor receptor 2 (VEGFR2), and it showed tolerance to a single-agent toxicity profile [12,13]. In 2014, apatinib was approved by the Chinese State Food and Drug Administration for the treatment of chemotherapy-refractory gastric cancer [14]. It also manifested satisfactory efficacy among patients with NSCLC [15]. Emerging data demonstrated that vascular endothelial growth factor (VEGF)/VEGFR2, which is a pro-angiogenic factor, not only plays a critical role in promoting tumor angiogenesis but also participates in modulating tumor-induced immunosuppression (accumulation of Tregs, MDSC, and immature dendritic cells) that enables the tumor to evade host immunosurveillance [16]. Therefore, we here hypothesize that apatinib may have the ability to change the tumor tolerogenic microenvironment.

This study addressed the issue of whether SABR-elicited antitumor immunity could be significantly enhanced with a

novel TKI-apatinib, then further leading to the suppression of both irradiated and nonirradiated (primary and secondary tumor, respectively) tumor growth.

Materials and Methods

1. Cell lines and animals

Mouse-derived Lewis lung carcinoma (LLC) cells and colon adenocarcinoma cell line (MC38) were purchased from American Type Culture Collection (ATCC) and cultured as described [8]. C57BL/6 mice (male, 4- to 5-week-old) were purchased from Vital River Laboratory Animal Technology Co., Ltd. (Beijing, China).

2. Tumor challenge and treatment

C57BL/6 mice were injected subcutaneously with LLC cells or MC38 cells as indicated in each experiment. Tumor volumes were calculated as $\text{length} \times \text{width}^2 \times 0.5$. Before irradiation, all mice were lightly anesthetized by intraperitoneal injection of propofol (150 mg/kg). Then, mice were positioned on a customized restraining device, and the whole body was protected by lead shielding except for the tumor area to be irradiated. Mice received a single dose of 15 Gy at a rate of 600 cGy/min using 12 MeV electrons with Siemens Oncor Impression (Siemens Medical Systems, Concord, CA). Apatinib was provided by Hengrui Pharmaceutical Group Co. Ltd. (Lianyungang, China) and administered by intragastric administration (i.g.) to mice once a day and for a total of 7 days.

3. Immunohistochemical staining

Immunohistochemistry was performed as previously described [17]. Sections were incubated with primary antibodies overnight at 4°C, including phospho-STAT3 (p-STAT3), CD4, CD8, p-VEGFR2, hypoxia-inducible factor-1 α , and PD-L1 (all from Cell Signaling Technology, MA). Then, the sections were incubated with the secondary horseradish peroxidase conjugated antibody (Absin, Shanghai, China) for 30 minutes at room temperature. Targeted proteins were visualized with diami-nobenzidine (Zhongshan Golden Bridge, Beijing, China). Five random fields were selected for estimating the staining intensities by three independent observers individually.

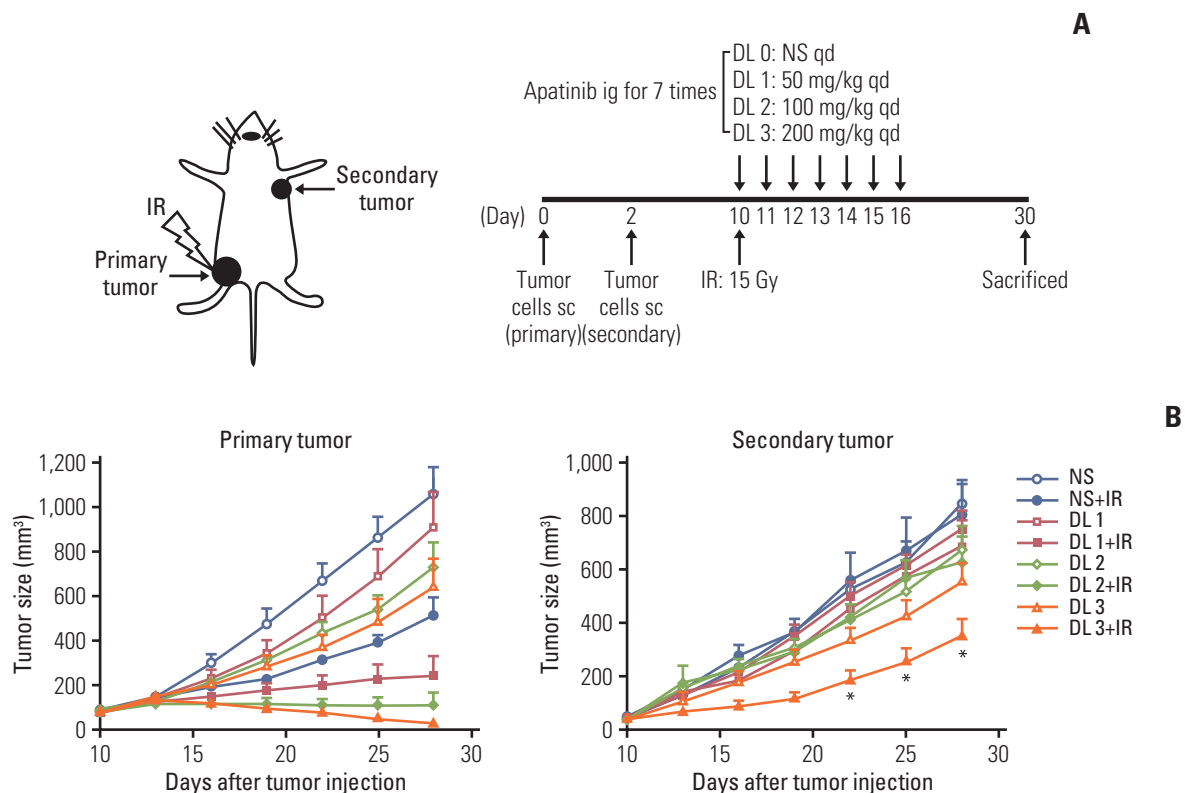


Fig. 1. High dose of apatinib synergizes with stereotactic ablative radiotherapy in the Lewis lung carcinoma (LLC) mouse model. (A) C57BL/6 mice were injected subcutaneously with 5×10^5 LLC cells in the left hindlimb (primary tumor; irradiated) on day 0, and in the right flank (secondary tumor; nonirradiated) on day 2. On day 10, mice were administered intragastrically with varying doses of apatinib (NS; dose level [DL] of 50 mg/kg, 150 mg/kg, and 200 mg/kg) daily for 7 days. A single dose of 15 Gy radiotherapy to the primary tumor was administered to half of the mice in each DL group on day 10. Tumor growth was evaluated every 3 days until day 30. (B) Tumor growth delay of primary tumors (left) and secondary tumors (right) in mice. Representative data are shown from two experiments conducted with five mice per group. * $p < 0.05$, ** $p < 0.01$. IR, irradiation; NS, normal saline; qd, once daily; sc, subcutaneous administration.

4. Flow cytometric analysis

To obtain single-cell suspensions, the spleen was first scraped with scissors, and the homogenate was then passed through a $0.45 \mu\text{m}$ nylon mesh. Separated splenocytes were immuno-stained with anti-mouse CD3, CD4, CD8, Foxp3, and CD25 (all from BD Pharmingen, San Diego, CA) for 30 minutes at 4°C . Samples were collected on a FACSCalibur Flow Cytometer (BD Pharmingen), and data were analyzed with FlowJo software (BD Biosciences, San Diego, CA). An example of the gating strategy used for selection of CD4^+ and CD8^+ T cells and $\text{CD4}^+ \text{CD25}^+ \text{Foxp3}^+$ Tregs cells is presented in S1 Fig.

5. Interferon- γ ELISPOT assay and enzyme-linked immunosorbent assay

Interferon γ (IFN- γ)-producing lymphocytes were detected with ELISPOT according to the manufacturer's instructions (Dakewe Biotech Co. Ltd., Shenzhen, China). Spleen single cells (2×10^5) from tumor-bearing mice were cultured with 2×10^3 LLC cells or MC38 cells in 96-well tissue culture plates precoated with an anti-IFN- γ antibody. Each positive spot represents an active lymphocyte. The supernatants were removed and stored at -80°C for further enzyme-linked immunosorbent assay against cytokines.

6. Statistical analysis

Data were analyzed with Prism 7.0 software (GraphPad Software, San Diego, CA). Data are represented as the mean \pm

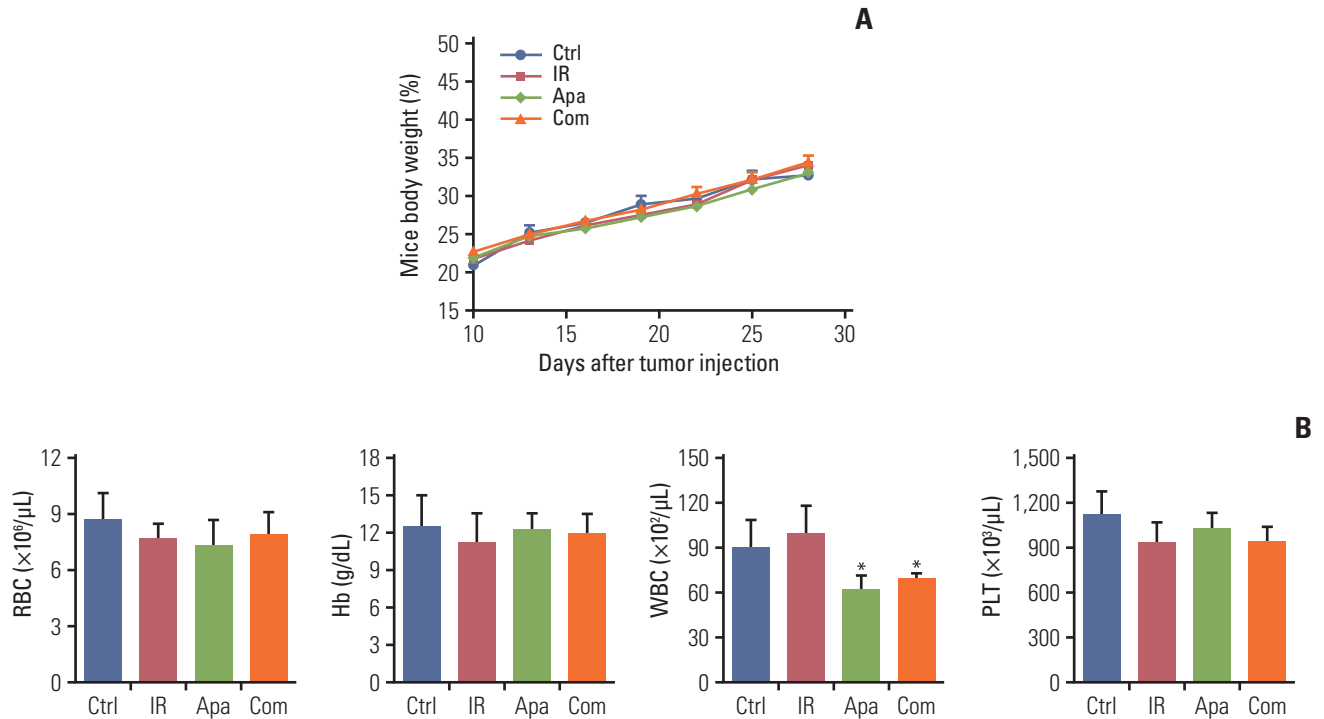


Fig. 2. Toxicity analysis for treatments with stereotactic ablative radiotherapy (SABR) and apatinib in C57/BL6 mice bearing Lewis lung carcinoma. (A) Total body weight of high-dose level (200 mg/kg) apatinib-treated plus SABR mouse groups was monitored every 3 days. (B) Blood analysis of mice after various treatments. * $p < 0.05$. (A, B) Representative data are shown from two experiments conducted with five mice per group. Ctrl, control; IR, irradiation; Apa, apatinib; Com, combination treatment; RBC, red blood cells; Hb, hemoglobin; WBC, white blood cells; PLT, platelets.

standard error of mean for all figures panels in which error bars are shown. Statistical analyses were carried out with Student's *t* test for two groups. For comparison among treatment groups, statistical analysis was performed using analysis of variance followed by Dunnett *t* test and log-rank test. The results were considered statistically significant at $p < 0.05$ and 0.01 .

7. Ethical statement

All animal experiments were performed according to protocols approved by the Institutional Animal Care and Use Committee of Xuzhou Medical University.

Results

1. Apatinib synergizes with SABR in the LLC mouse model

Previous research indicated that apatinib was able to downregulate the PD-L1 expression through the inactivation of STAT3 [18,19]. In this study, we found that the PD-L1 expression of LLC cell could be reduced by apatinib in a dose-dependent manner (S2A Fig.). As shown in S2B Fig., when VEGFR2 was activated by vascular endothelial growth factor (VEGF) as evidenced by increased p-VEGFR2 level, the expression of p-STAT3 and PD-L1 was elevated, and the total STAT3 expression was unchanged. Additionally, the elevation of PD-L1 was neutralized after deactivating STAT3 by S3I-201, an inhibitor of STAT3. These results suggested that apatinib could downregulate PD-L1 expression through VEGFR2/STAT3 pathway.

It has been proved that PD-1/PD-L1 axis restrains the effect of SABR [10,11,20], the function of apatinib on the SABR treatment was further examined in a LLC mouse

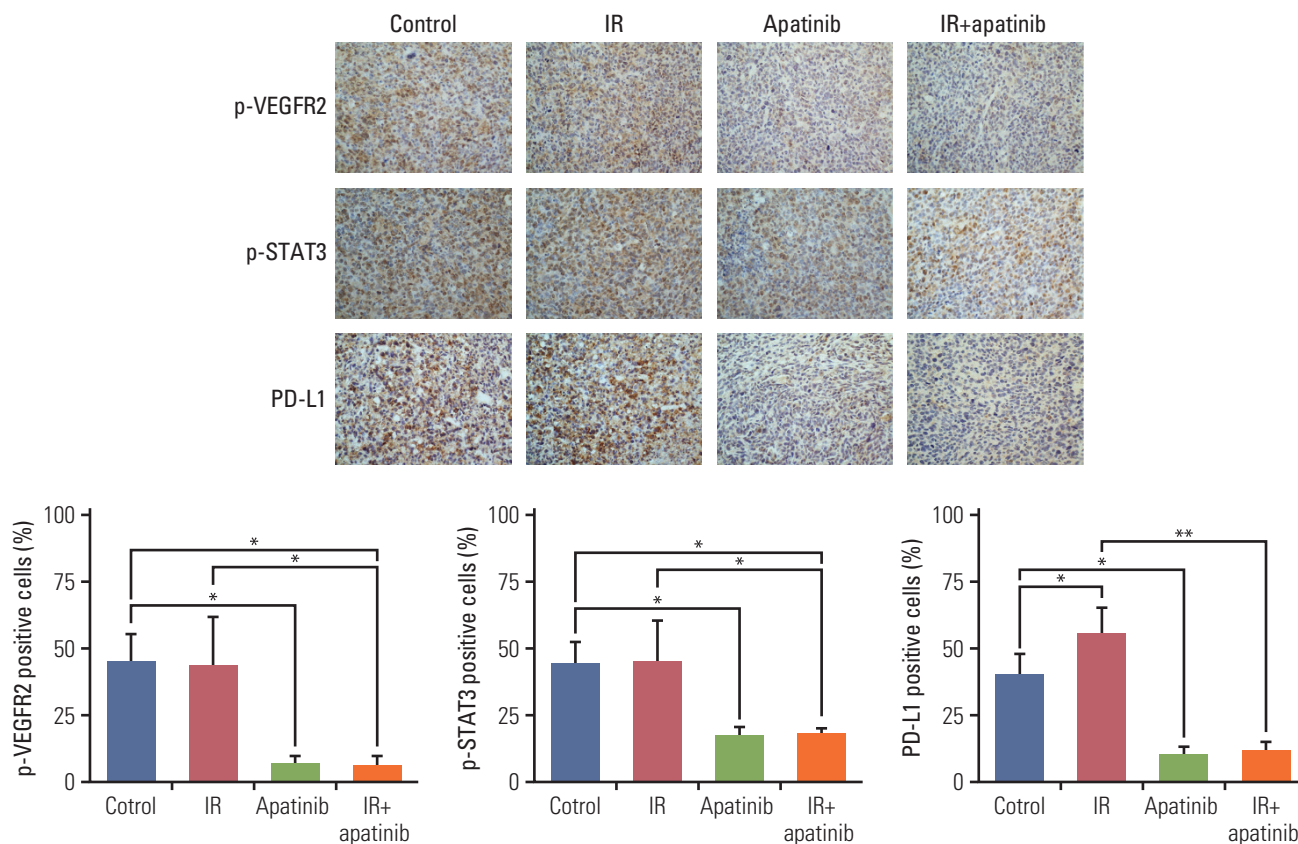


Fig. 3. Increased programmed death-ligand 1 (PD-L1) expression in nonirradiated tumor tissue following stereotactic ablative radiotherapy could be overcome by concurrent apatinib therapy. The expression levels of PD-L1, phospho-vascular endothelial growth factor receptor 2 (VEGFR2), and phospho-STAT3 in nonirradiated tumor were detected by immunohistochemical ($\times 40$). Representative data are shown from two experiments conducted with five mice per group. * $p < 0.05$, ** $p < 0.01$. IR, irradiation.

model. LLC cells were injected into C57BL/6 mice at two separate sites as illustrated (Fig. 1A). For the single 15 Gy modality without apatinib, tumor growth delay was observed only at the irradiated lesion (primary tumor). When SABR and apatinib were combined, significant retardation of primary tumor growth could be observed. Especially, the growth of secondary tumor volume was different between SABR plus apatinib of 200 mg/kg group and apatinib 200 mg/kg group ($p < 0.05$) (Fig. 1B); however, all the secondary tumors in these two groups were not received radiotherapy, while the primary tumors in the combined group received radiotherapy, indicating that the irradiation of the primary tumor had an impact (abscopal effect) on the tumor shrinkage of the secondary tumor.

In the toxicity analysis, we found that ionizing radiation combined with apatinib 200 mg/kg did not lead to significant weight loss or treatment-related death (Fig. 2A). Blood analysis was performed on day 30 when the mice were sac-

rificed. The results showed a trend toward mildly reduced frequency of white blood cells counts in mice treated with both single modality of apatinib (200 mg/kg) and combined strategy with SABR, without showing any other myelosuppressive toxicity (Fig. 2B).

2. Increased PD-L1 expression in tumor tissue following SABR could be overcome by concurrent apatinib therapy

The mechanism underlying the enhanced antitumor effects of SABR mediated by apatinib was further explored. We investigated whether PD-L1 expression could be down-regulated with apatinib treatment *in vivo*. PD-L1 expression of irradiated tumors was significantly greater after SABR ($p < 0.01$) (S3 Fig.). Interestingly, an increased expression of PD-L1 was also observed on nonirradiated secondary tumors after irradiation, compared with those of observed in control group ($p < 0.05$) (Fig. 3). However, both of which were

A

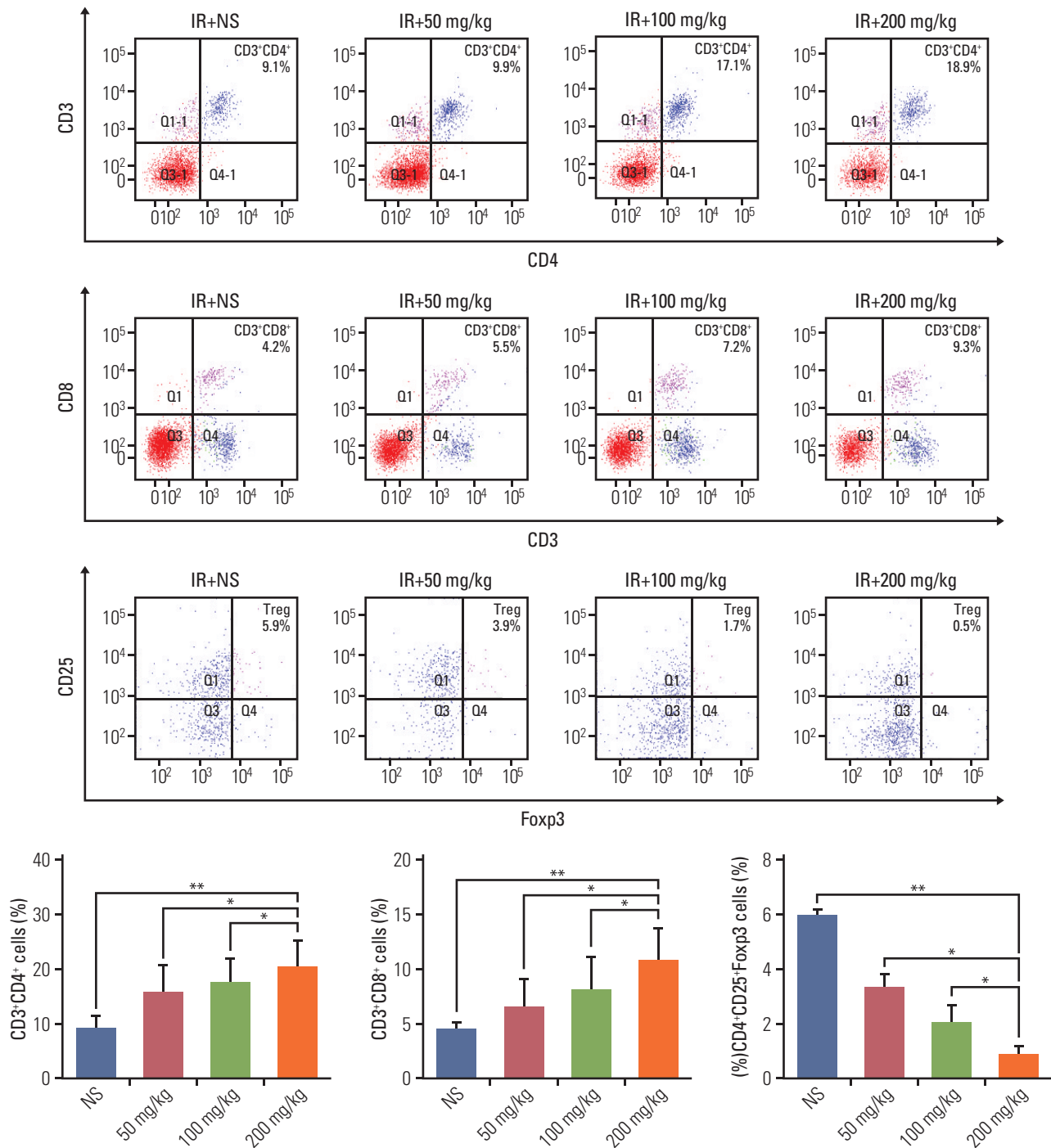


Fig. 4. The combination of apatinib and stereotactic ablative radiotherapy could modulate the composition of immune cells, elicit tumor-specific T-cell activation and result in varied cytokine expression profiles. (A) The lymphocyte population in the spleen of tumor-bearing mice were assessed by flow cytometry. NS, normal serum. (Continued to the next page)

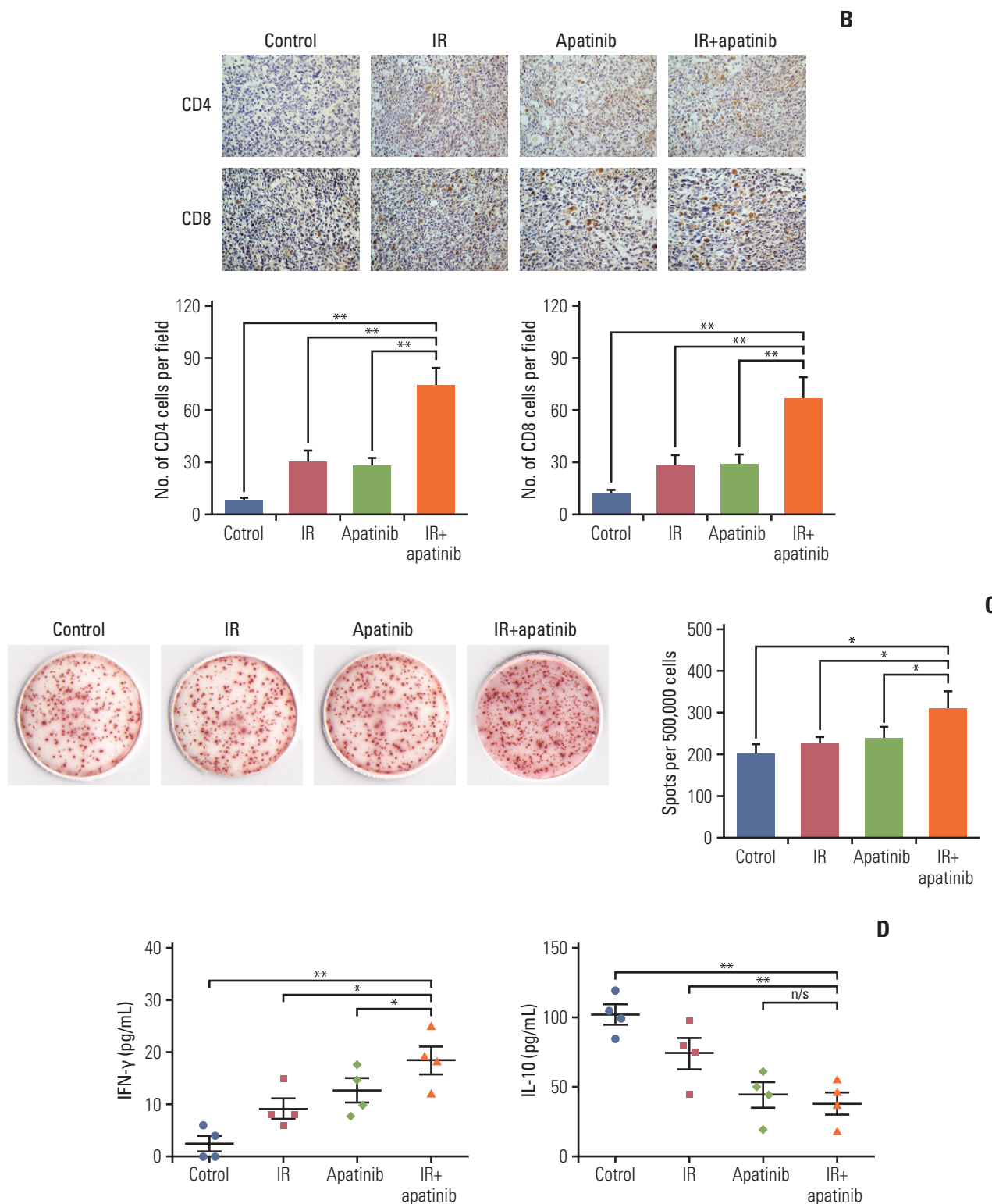


Fig. 4. (Continued from the previous page) (B) The CD4⁺ and CD8⁺ tumor-infiltrating lymphocytes in the secondary tumors were stained by immunohistochemical (×40). (C, D) Interferon γ (IFN- γ)-producing lymphocytes from spleen single cells were detected with ELISPOT assay; the supernatants were removed and stored at -80°C for further cytokine detection with enzyme-linked immunosorbent assay. IR, irradiation. * $p < 0.05$, ** $p < 0.01$, n/s, no significant. (A-D) Representative data are shown from three experiments conducted with five mice per group.

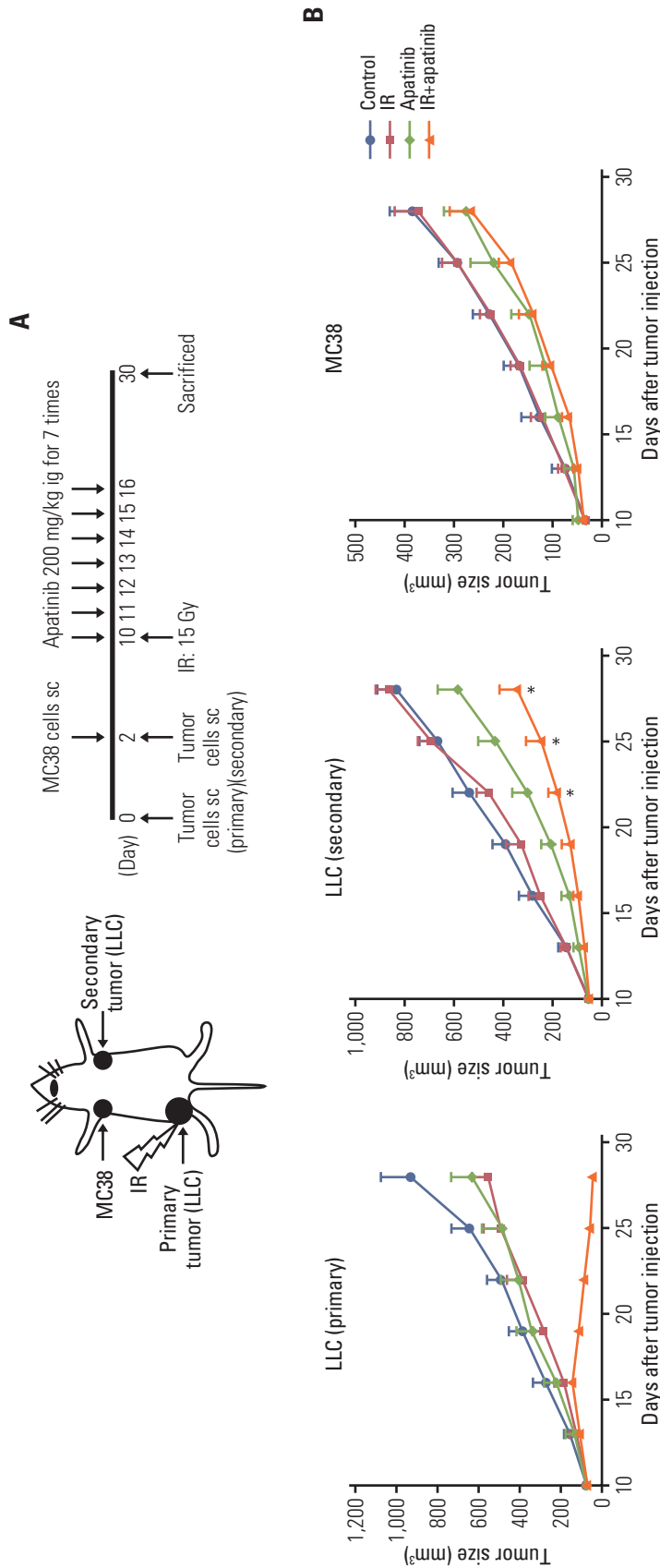


Fig. 5. Combination radiotherapy and apatinib therapy evoked tumor antigen-specific immune responses. (A) Mice were injected subcutaneously with 5×10^5 Lewis lung carcinoma (LLC) cells in the left hindlimb (primary tumor; irradiated) on day 0, and in the right flank (secondary tumor; nonirradiated) on day 2. The third-party tumor cells (MC38) were inoculated subcutaneously with 5×10^5 cells in the left flank (nonirradiated) on day 2. Apatinib 200 mg/kg was administered intragastrically to mice from day 10 to 16 for 7 times and primary LLC was administered as a single 15-Gy dose. (B) Tumor growth delay of primary LLC (left), secondary LLC (middle) and secondary MC38 tumor (right). IR, irradiation; ig, intragastric administration; sc, subcutaneous administration. (Continued to the next page)

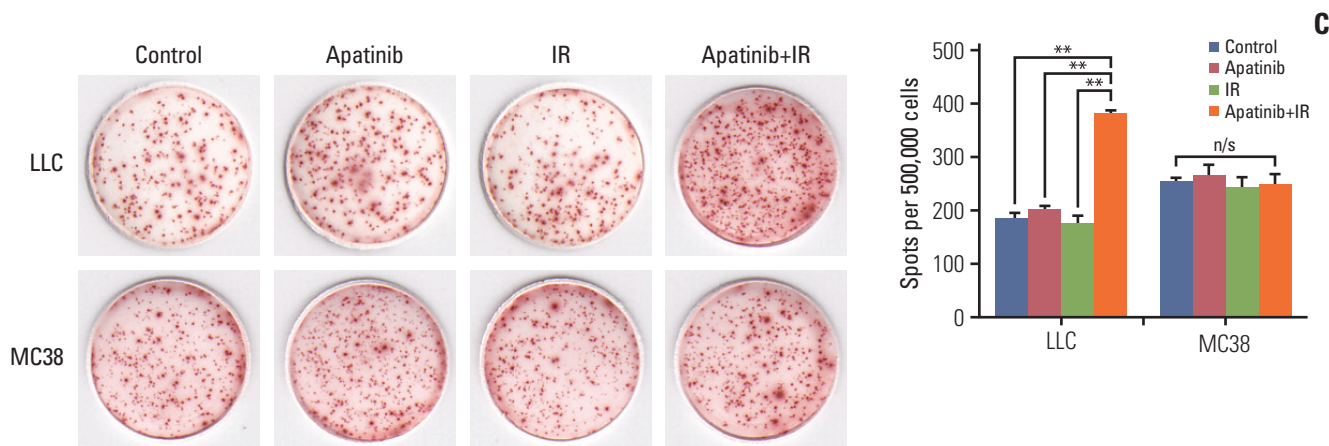


Fig. 5. (Continued from the previous page) (C) The number of interferon- γ -producing lymphocytes response to LLC or MC38 cells was detected with ELISPOT assay. * $p < 0.05$, ** $p < 0.01$, n/s, no significant. (B, C) Representative data are shown from two experiments conducted with five mice per group.

reversed by additional apatinib therapy through reduced the phosphorylation levels of VEGFR2 and STAT3 (Fig. 3, S3 Fig.). Therefore, the result partially explains the synergistic mechanism of the combined radiotherapy and apatinib strategy.

3. Apatinib combined with SABR could modulate the composition of immune cells and elicit activation of T lymphocyte

Subsequently, the lymphocyte population in the spleens of tumor-bearing mice was assessed. We found that the overall percentage of CD4⁺ and CD8⁺ T cells was significantly increased with the increase of apatinib dose. However, the percentage of CD4⁺ CD25⁺ Foxp3⁺ Tregs was significantly decreased, all in a dose-dependent fashion (Fig. 4A). Analysis of the presence of tumor-infiltrating lymphocytes (TILs) in secondary tumors indicated that, treatment with concurrent SABR and apatinib led to a significant increase in CD4⁺ and CD8⁺ TILs ($p < 0.01$, compared with all other groups) (Fig. 4B). ELISPOT assay showed that the number of activated IFN- γ -secreted lymphocyte was significantly greater only in mice receiving combined treatment ($p < 0.05$, compared with all other single groups) (Fig. 4C). The overall level of IFN- γ secreted from splenic lymphocytes was significantly greater in combination therapy, compared with that of single apatinib or SABR treatment (Fig. 4D, left). On the contrary, interleukin 10, which was involved in tumor-mediated immune suppression, was significantly decreased in the combined group (Fig. 4D, right).

Collectively, these results suggest that apatinib with combined SABR can modify the tumor microenvironment that

may be associated with tumors outside the radiation field rejection.

4. Combined radiotherapy and apatinib therapy evoked tumor antigen-specific immune responses

To demonstrate that the applicability of combined SABR and apatinib therapy is tumor antigen-specific, LLC cells were injected into C57BL/6 mice as primary and secondary tumors and MC38 were injected as the third experimental tumor. Primary LLC were given a single dose of 15 Gy (Fig. 5A). Consistent with previous results, in both the primary irradiated and secondary nonirradiated LLC tumor sites, slowed tumor progression could be significantly induced with SABR in combination with apatinib (Fig. 5B). However, there was no difference in efficacy of MC38 tumor growth in the combined therapy group over apatinib single-agent therapy ($p > 0.05$) (Fig. 5B). For the response to LLC, the number of IFN- γ -producing lymphocytes in the combination treatment group was significantly higher than in the other three groups. However, for MC38, the positive spots counts were not affected by SABR, apatinib, or the combination therapy (Fig. 5C). From these observations, we conclude that the antitumor abscopal effect induced by combination radiotherapy and apatinib was tumor antigen-specific.

5. Apatinib and radiotherapy treated tumor-bearing mice were resistant to tumor rechallenge and presented improved long-term survival

To facilitate a broader application of this novel simultaneous strategy, we next investigated whether this combination

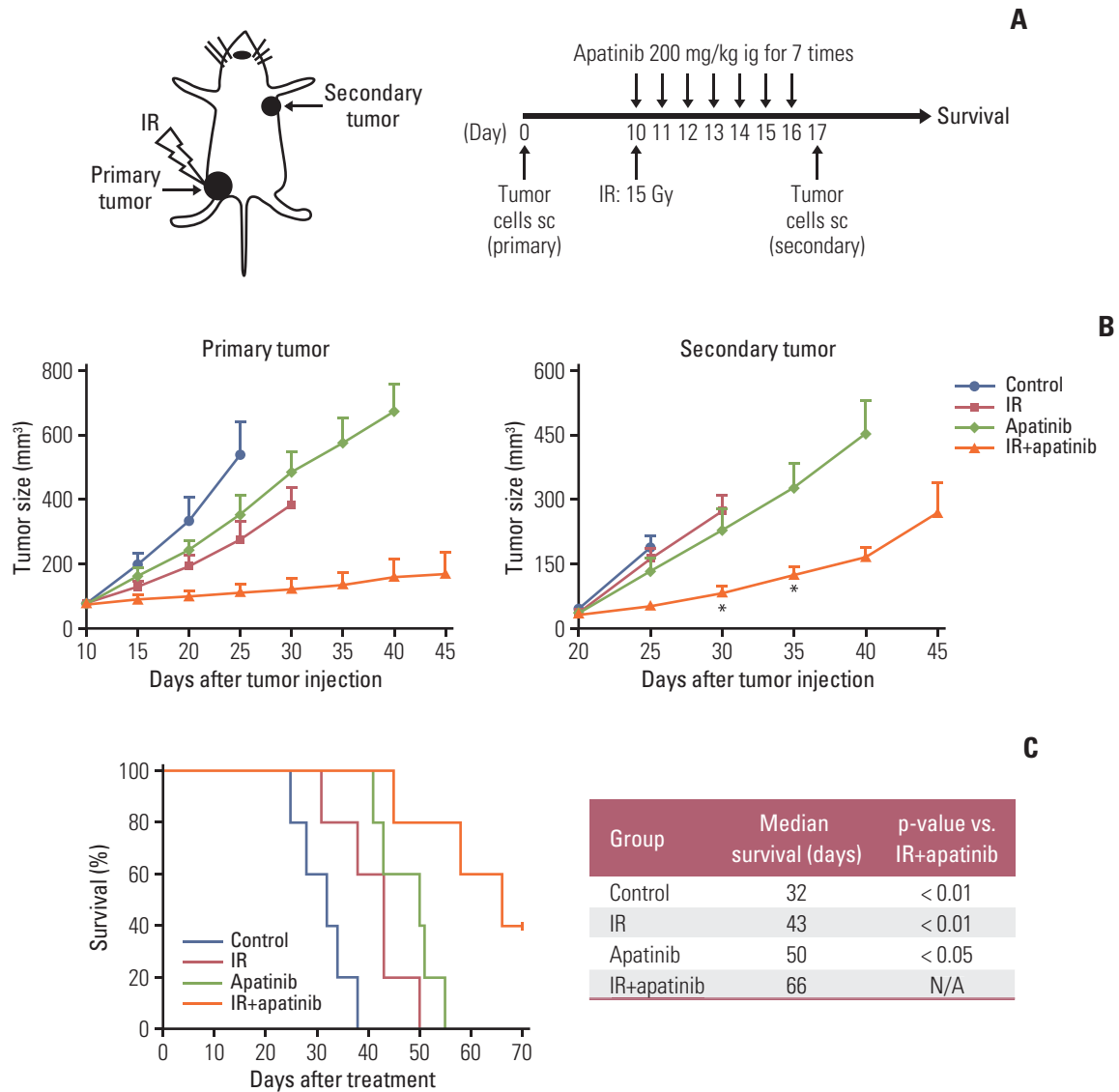


Fig. 6. Tumor-bearing mice with combined stereotactic ablative radiotherapy and apatinib treatment were not only resistant to the tumor rechallenge but also improving long-term survival. (A) Lewis lung carcinoma (LLC) cells (5×10^5) were injected in the left hindlimb as primary tumor, after all the treatments finished, mice were rechallenged with LLC cells (5×10^5) on the opposite flank. (B) Tumor growth delay of primary tumor (left) and secondary rechallenge tumor (right). * $p < 0.05$, ** $p < 0.01$. (C) Kaplan-Meier survival curves and life table for LLC bearing mice. (B, C) Representative data are shown from two experiments conducted with five mice per group. IR, irradiation; ig, intragastric administration; sc, subcutaneous administration; N/A, not available.

therapy could prevent metastasis and further increase survival. LLC cells were injected in the left hindlimb as primary tumor. After all the treatments were complete, mice were rechallenged with LLC cells on the opposite flank. Both tumor growth and survival time were monitored (Fig. 6A). As shown in Fig. 5B, for rechallenged tumors, SABR or apatinib therapy alone showed negligible inhibition of tumor growth compared with that of control group. However,

when SABR was combined with apatinib, tumor growth was much slower than that of in other groups (Fig. 6B). As for survival analysis, survival could be more effectively improved with the combined treatment of radiation therapy and apatinib, and 40% of mice were still alive until the end of the experiment (Fig. 6C). Together, these results suggest that the two-pronged regimen could not only prevent tumor metastasis but also prolong the survival time in tumor-bearing mice.

Discussion

Our proof-of-principle study suggested that, apatinib, a novel VEGFR2 TKI, may modulate the tumor microenvironment, not only by reversing the PD-L1 expression increased by SABR but also by changing other constituents. Especially at a high dose, apatinib worked in a synergistic manner with SABR, and induced an abscopal effect. In addition, we demonstrated that SABR-induced antitumor immunity was tumor antigen-specific, and the combined SABR and apatinib therapy could resistant to tumor rechallenge, thereby extending survival time.

Many studies have shown that VEGFA/VEGFR2 is not only a pivotal growth factor that promotes angiogenesis but also directly supports cancer cell growth through an autocrine-positive feedback loop [21]. Apatinib (YN968D1) is a novel and highly selective competitor for the ATP binding site of VEGFR2 tyrosine kinase, and it blocks downstream signaling transduction [12]. Thus, apart from the anti-angiogenic effect, apatinib may directly inhibit tumor cells or affect other cells expressing VEGFR as a cytotoxic agent [12,22].

PD-L1 is expressed on many types of cells, including T cells, B cells, monocytes, and tumor cells, which suppresses T-cell function and results in immune escape by binding to PD-1 [23]. STAT3, a point of convergence for numerous tyrosine kinases (including VEGFR, platelet-derived growth factor receptor, epidermal growth factor receptor, and Src) in diverse cancer types including NSCLC [22,24]. STAT3 could bind to the PD-L1 promoter to regulate its expression transcriptionally [25]. It has been previously demonstrated that there was a significant correlation between PD-L1 and VEGFR2 expression in tumor cells and PD-L1 expression could be inhibited with apatinib by targeting STAT3 [18,19]. These results were consistent with our findings (Fig. 2, S2 and S3 Figs.).

Recent studies have reported that VEGFR2 is also selectively expressed on Tregs and can directly induce proliferation [26]. Drugs with anti-angiogenic properties can also counteract the proliferation of tumor-induced immunosuppressive cells. Sunitinib, another TKI-targeted VEGFR family, has been found to be able to decrease the number of Tregs in a dose-dependent fashion in colon-tumor-bearing mice [27]. It demonstrated that VEGF could directly suppress T-cell proliferation and activation via binding to VEGFR2 [28]. In this study, we found that the overall percentage of CD4⁺ and CD8⁺ T cells in the spleen could be significantly increased with apatinib, and the infiltration of T cells into the tumor could also be improved (Fig. 4A and B). This better infiltration could also be associated with the capacity of anti-angiogenic molecules to normalize tumor vasculature and pre-

ferentially promote infiltration of immune effector cells into the tumor parenchyma [29].

Increased evidence and our study indicated that SABR-induced a local inflammatory response that could enhance the infiltration of T lymphocyte and simultaneously induce PD-L1 expression in the tumor microenvironment (Fig. 3), which markedly weakens SABR-induced antitumor immunity. Based on the comprehensive immuno-modulatory capacity, anti-angiogenic molecules may be sufficient to enhance the systemic antitumor immunity mediated by SABR, especially at the sites remote from irradiation. This is the first report on apatinib—a novel anti-angiogenic drug—combined with SABR that elicited a curative abscopal effect. In addition, we also found that the antitumor abscopal effect induced by our dual therapy was tumor antigen-specific (Fig. 5C). This observation is consistent with the hypothesis that radiotherapy has the potential to trigger immunogenic tumor-cell death and induce danger signals that effectively exposes tumor-specific antigen, contributing to the phenomenon referred to as “*in situ*” vaccination [2]. Moreover, our study suggested herein that this novel dual therapy could protect tumor-bearing mice from tumor rechallenge. In this way, survival time could be prolonged (Fig. 6).

The current radiotherapy dose and best fractionation have been empirically validated. It was suggested that optimal antitumor immunity could be induced with 8 Gy×3 fractionated doses instead of single-dose irradiation in the preclinical model [30]. However, this is a sub-curative dose, we chose a single 15 Gy dose in our experiment and combined it with 200 mg/kg apatinib therapy, without increasing additional toxicity (Fig. 2). Park et al. [11] previously applied 15 Gy×1 irradiation regimen in animal models, without showing apparent toxicity and the effects on immune activation were superior to a 3 Gy×5 fractionated strategy.

In summary, our results suggested that apatinib could be synergistically applied with SABR to enhance the systemic antitumor efficacy through modifying tumor microenvironment. Moreover, our findings could broaden the scope of current strategy to reverse the immunosuppressive tumor environment and provide insights into rational design of clinical trials.

Electronic Supplementary Material

Supplementary materials are available at Cancer Research and Treatment website (<https://www.e-crt.org>).

Conflicts of Interest

Conflict of interest relevant to this article was not reported.

Acknowledgments

This work was supported by National Natural Science Foundation of China grants 81472792 and 81702813, Postgraduate Research &

Practice Innovation Program of Jiangsu Province grants SJCX18_0707 and SJCX19_0766, and the Technology Office Foundation of Lianyungang City (No. SH1613).

References

- Jaffray DA. Image-guided radiotherapy: from current concept to future perspectives. *Nat Rev Clin Oncol*. 2012;9:688-99.
- Herrera FG, Bourhis J, Coukos G. Radiotherapy combination opportunities leveraging immunity for the next oncology practice. *CA Cancer J Clin*. 2017;67:65-85.
- Postow MA, Callahan MK, Barker CA, Yamada Y, Yuan J, Kitano S, et al. Immunologic correlates of the abscopal effect in a patient with melanoma. *N Engl J Med*. 2012;366:925-31.
- Siva S, Callahan J, MacManus MP, Martin O, Hicks RJ, Ball DL. Abscopal [corrected] effects after conventional and stereotactic lung irradiation of non-small-cell lung cancer. *J Thorac Oncol*. 2013;8:e71-2.
- Stamell EF, Wolchok JD, Gnjatich S, Lee NY, Brownell I. The abscopal effect associated with a systemic anti-melanoma immune response. *Int J Radiat Oncol Biol Phys*. 2013;85:293-5.
- Wersäll PJ, Blomgren H, Pisa P, Lax I, Kalkner KM, Svedman C. Regression of non-irradiated metastases after extracranial stereotactic radiotherapy in metastatic renal cell carcinoma. *Acta Oncol*. 2006;45:493-7.
- Fridman WH, Pages F, Sautes-Fridman C, Galon J. The immune contexture in human tumours: impact on clinical outcome. *Nat Rev Cancer*. 2012;12:298-306.
- Son CH, Bae JH, Shin DY, Lee HR, Jo WS, Yang K, et al. Combination effect of regulatory T-cell depletion and ionizing radiation in mouse models of lung and colon cancer. *Int J Radiat Oncol Biol Phys*. 2015;92:390-8.
- Golden EB, Chhabra A, Chachoua A, Adams S, Donach M, Fenton-Kerimian M, et al. Local radiotherapy and granulocyte-macrophage colony-stimulating factor to generate abscopal responses in patients with metastatic solid tumours: a proof-of-principle trial. *Lancet Oncol*. 2015;16:795-803.
- Deng L, Liang H, Burnette B, Beckett M, Darga T, Weichselbaum RR, et al. Irradiation and anti-PD-L1 treatment synergistically promote antitumor immunity in mice. *J Clin Invest*. 2014;124:687-95.
- Park SS, Dong H, Liu X, Harrington SM, Krco CJ, Grams MP, et al. PD-1 restrains radiotherapy-induced abscopal effect. *Cancer Immunol Res*. 2015;3:610-9.
- Tian S, Quan H, Xie C, Guo H, Lu F, Xu Y, et al. YN968D1 is a novel and selective inhibitor of vascular endothelial growth factor receptor-2 tyrosine kinase with potent activity in vitro and in vivo. *Cancer Sci*. 2011;102:1374-80.
- Li J, Zhao X, Chen L, Guo H, Lv F, Jia K, et al. Safety and pharmacokinetics of novel selective vascular endothelial growth factor receptor-2 inhibitor YN968D1 in patients with advanced malignancies. *BMC Cancer*. 2010;10:529.
- Li J, Qin S, Xu J, Xiong J, Wu C, Bai Y, et al. Randomized, double-blind, placebo-controlled phase iii trial of apatinib in patients with chemotherapy-refractory advanced or metastatic adenocarcinoma of the stomach or gastroesophageal junction. *J Clin Oncol*. 2016;34:1448-54.
- Zhang L, Shi M, Huang C, Liu X, Xiong JP, Chen G, et al. A phase II, multicenter, placebo-controlled trial of apatinib in patients with advanced nonsquamous non-small cell lung cancer (NSCLC) after two previous treatment regimens. *J Clin Oncol*. 2012;30(15 Suppl):7548.
- Voron T, Marcheteau E, Pernot S, Colussi O, Tartour E, Taieb J, et al. Control of the immune response by pro-angiogenic factors. *Front Oncol*. 2014;4:70.
- Jiang XD, Dai P, Wu J, Song DA, Yu JM. Inhibitory effect of radiotherapy combined with weekly recombinant human endostatin on the human pulmonary adenocarcinoma A549 xenografts in nude mice. *Lung Cancer*. 2011;72:165-71.
- Zheng B, Ren T, Huang Y, Guo W. Apatinib inhibits migration and invasion as well as PD-L1 expression in osteosarcoma by targeting STAT3. *Biochem Biophys Res Commun*. 2018;495:1695-701.
- Qiu MJ, He XX, Bi NR, Wang MM, Xiong ZF, Yang SL. Effects of liver-targeted drugs on expression of immune-related proteins in hepatocellular carcinoma cells. *Clin Chim Acta*. 2018;485:103-5.
- Liu Y, Dong Y, Kong L, Shi F, Zhu H, Yu J. Abscopal effect of radiotherapy combined with immune checkpoint inhibitors. *J Hematol Oncol*. 2018;11:104.
- Peng S, Zhang Y, Peng H, Ke Z, Xu L, Su T, et al. Intracellular autocrine VEGF signaling promotes EBDC cell proliferation, which can be inhibited by Apatinib. *Cancer Lett*. 2016;373:193-202.
- Liu K, Ren T, Huang Y, Sun K, Bao X, Wang S, et al. Apatinib promotes autophagy and apoptosis through VEGFR2/STAT3/BCL-2 signaling in osteosarcoma. *Cell Death Dis*. 2017;8:e3015.
- Sun C, Mezzadra R, Schumacher TN. Regulation and function of the PD-L1 checkpoint. *Immunity*. 2018;48:434-52.
- Yu H, Jove R. The STATs of cancer: new molecular targets come of age. *Nat Rev Cancer*. 2004;4:97-105.
- Chen J, Jiang CC, Jin L, Zhang XD. Regulation of PD-L1: a novel role of pro-survival signalling in cancer. *Ann Oncol*. 2016;27:409-16.
- Terme M, Pernot S, Marcheteau E, Sandoval F, Benhamouda N, Colussi O, et al. VEGFA-VEGFR pathway blockade inhibits

- tumor-induced regulatory T-cell proliferation in colorectal cancer. *Cancer Res.* 2013;73:539-49.
27. Ozao-Choy J, Ma G, Kao J, Wang GX, Meseck M, Sung M, et al. The novel role of tyrosine kinase inhibitor in the reversal of immune suppression and modulation of tumor microenvironment for immune-based cancer therapies. *Cancer Res.* 2009;69:2514-22.
28. Ziogas AC, Gavalas NG, Tsiatas M, Tsitsilonis O, Politi E, Terpos E, et al. VEGF directly suppresses activation of T cells from ovarian cancer patients and healthy individuals via VEGF receptor Type 2. *Int J Cancer.* 2012;130:857-64.
29. Tian L, Goldstein A, Wang H, Ching Lo H, Sun Kim I, Welte T, et al. Mutual regulation of tumour vessel normalization and immunostimulatory reprogramming. *Nature.* 2017;544:250-4.
30. Dewan MZ, Galloway AE, Kawashima N, Dewyngaert JK, Babb JS, Formenti SC, et al. Fractionated but not single-dose radiotherapy induces an immune-mediated abscopal effect when combined with anti-CTLA-4 antibody. *Clin Cancer Res.* 2009;15:5379-88.